Measurements beneath an Antarctic ice shelf using an autonomous underwater vehicle

K. W. Nicholls,[1] E. P. Abrahamsen,[1] J. J. H. Buck,[2] P. A. Dodd,[3] C. Goldblatt,[3] G. Griffiths,[4] K. J. Heywood,[3] N. E. Hughes,[5] A. Kaletzky,[6] G. F. Lane-Serff,[2] S. D. McPhail,[4] N. W. Millard,[4] K. I. C. Oliver,[3] J. Perrett,[4] M. R. Price,[3] C. J. Pudsey,[1] K. Saw,[4] K. Stansfield,[4] M. J. Stott,[7] P. Wadhams,[6] A. T. Webb,[4] and J. P. Wilkinson[5]

Received 16 February 2006; revised 16 March 2006; accepted 21 March 2006; published 29 April 2006.

[1] The cavities beneath Antarctic ice shelves are among the least studied regions of the World Ocean, yet they are sites of globally important water mass transformations. Here we report results from a mission beneath Fimbul Ice Shelf of an autonomous underwater vehicle. The data reveal a spatially complex oceanographic environment, an ice base with widely varying roughness, and a cavity periodically exposed to water with a temperature significantly above the surface freezing point. The results of this, the briefest of glimpses of conditions in this extraordinary environment, are already reforming our view of the topographic and oceanographic conditions beneath ice shelves, holding out great promises for future missions from similar platforms. **Citation:** Nicholls, K. W., et al. (2006), Measurements beneath an Antarctic ice shelf using an autonomous underwater vehicle, *Geophys. Res. Lett.*, *33*, L08612, doi:10.1029/2006GL025998.

1. Introduction

[2] Ice shelves are the floating extension of the Antarctic Ice Sheet and they fringe much of continental Antarctica. They are often in excess of 1500 m thick [*Lythe and Vaughan*, 2001], and can be several hundred thousand square kilometers in area. As they are afloat, the bases of Antarctic ice shelves constitute an intimate link between the ice sheet and the Southern Ocean, and the very cold water masses formed within some sub-ice shelf cavities cool and freshen the deep waters supplied to the World Ocean [*Orsi et al.*, 2002]. Ice shelves also form the seaward boundary of the Antarctic Ice Sheet, with changes in ice shelf melt rate, for example, affecting the rate of discharge of inland ice, and therefore global sea level [*Payne et al.*, 2004]. In these ways, ice shelves and the processes beneath them form an integral component of the climate system: for a full description of the climate system and its likely response to man-made changes, these processes must in some way be incorporated within global climate models.

[3] Advancing our understanding of oceanographic processes beneath ice shelves has long been hampered by the difficulty in accessing the sub-ice shelf cavities to make measurements. Boreholes through the ice allow essentially point measurements [*Nicholls and Makinson*, 1998], and the logistical costs involved have meant that fewer than 20 access points have been made across all of Antarctica's ice shelves. Making further progress in understanding ice shelf-ocean interaction requires spatially extensive observations to complement the time series from borehole-deployed oceanographic moorings.

[4] On 13 February 2005 Autosub, an oceanographic autonomous underwater vehicle [*Millard et al.*, 1998] recently modified for missions into cavities beneath ice shelves [*Jones et al.*, 2005], was deployed beneath Fimbul Ice Shelf, Antarctica (Figure 1). Fed largely by Jutulstraumen, one of the principal ice streams of Dronning Maud Land, Fimbul Ice Shelf is characterized by having an ice tongue that overhangs the continental shelf break and slope, allowing that part of the ice shelf to come into contact with the relatively warm off-shelf waters. The cavity beneath the main ice shelf is up to 1000 m thick, with a series of sills connecting it to the Weddell Sea. The main sill, which largely underlies the ice tongue, is at 1°W. The next deepest sill, the eastern sill, is at 3°E [*Nøst*, 2004]. The vehicle flew a simple in and out mission that took it some 25 km into the sub-ice shelf cavity. Autosub flew at an elevation of 150 m above the seafloor, before turning around to exit the cavity on a reciprocal course but higher in the water column. For most of the return journey it flew in a terrain-following mode 100 m below the ice base (Figure 2a).

2. Basal Topography of the Ice Shelf

[5] The track taken by Autosub is shown in Figure 1, with the trajectory of the vehicle given in Figure 2a. For the return journey the upward-looking multibeam swath echosounder was within range of the ice surface, allowing a 3D acoustic image of the ice shelf basal topography to be obtained (Figure 3) [*Wadhams et al.*, 2006]. The first kilometer or so of the record shows the rather deeper drafting ice associated with the central portion of the ice shelf. For the remainder of the record the ice shelf base is at a depth of around 200 m and is a flat, almost specular reflector at the multibeam echosounder wavelength of

[1]British Antarctic Survey, Cambridge, UK.
[2]School of Mechanical, Aerospace and Civil Engineering, University of Manchester, Manchester, UK.
[3]School of Environmental Sciences, University of East Anglia, Norwich, UK.
[4]National Oceanography Centre, Southampton, UK.
[5]Scottish Society for Marine Sciences, Dunstaffnage Laboratory, Argyll, UK.
[6]Department of Applied Mathematics and Theoretical Physics, Centre for Mathematical Sciences, University of Cambridge, Cambridge, UK.
[7]Kent, UK.

0094-8276/06/2006GL025998$05.00

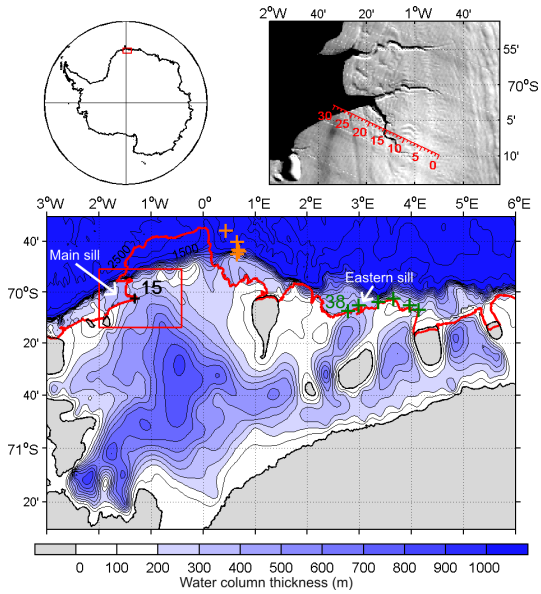

Figure 1. Map of Fimbul Ice Shelf showing water column thickness beneath the ice shelf and bathymetry seaward of the ice front. The red line indicates the ice front. Data are from a combination of the GEBCO-CE database, ship-based swath bathymetry from this cruise, and, for the ice-shelf covered region, seismic data [*Nøst*, 2004]. Contours are at 100-m intervals up to 1000 m depth, and then at 500-m intervals. Crosses show locations for CTD stations: black is CTD 15; orange are stations sampling possible inflow via main sill; green are stations sampling possible inflow via eastern sill. The inset figure is a MODIS visible satellite image from April 1st 2005 [*Scambos et al.*, 2005] with Autosub's return leg indicated in red. The contrast has been enhanced – the bottom of the rift at km-15 appears to be open water, but it is actually in shadow.

7.5 mm, but crossed by slightly shallower bands of dramatic topography with amplitudes and spatial wavelengths of around 20 m or so (Figure 3a). The satellite image (Figure 1) shows these bands to be associated with gentle surface depressions, known as flow traces [*Fahnestock et al.*, 2000]. If the ice shelf floats in hydrostatic equilibrium, depressions in the ice base will be typically nine times deeper than those at the surface. Ice base topography with spatial wavelengths substantially smaller than the ice thickness is not visible from satellites, as it does not survive to be reflected in the topography of the snow surface [*Raymond and Gudmundsson*, 2005]. There has therefore never before been any hint of the chaotic nature of the base beneath a flow trace. The past assumption has been that the surface depressions constituting flow traces reflect amplified, but similarly smooth depressions at the ice base. Such flow traces are ubiquitous on ice shelves, and so the present view that a typical ice-shelf base is for the most part smooth, with a drag coefficient that can be approximated by a constant value of around 0.003 [*MacAyeal*, 1984] needs to be reassessed. Clearly some areas of ice shelves are likely to exert very much higher drags on water flow, with consequences for the numerical models of sub-ice shelf ocean circulation [*Jenkins and Holland*, 2002] that will eventually supply parameterizations for global climate models.

3. Oceanographic Data

[6] The Acoustic Doppler Current Profiler (ADCP) data in Figure 2a show that, while the instruments performed as expected outside the cavity, their range dropped to a few tens of meters at best within a kilometer or two of moving beneath the ice shelf, and even those profiles suffered from a poor signal to noise ratio. To obtain the velocity vectors in Figure 2b, the median velocities from all the usable bins from both instruments (upward and downward) were averaged along the track in 1-km wide sections. Although the velocity data have been de-tided, the barotropic model used is not considered reliable near the topographic step imposed by the ice front, where, contrary to the vectors in Figure 2, other evidence strongly suggests that the entire water column is leaving the cavity.

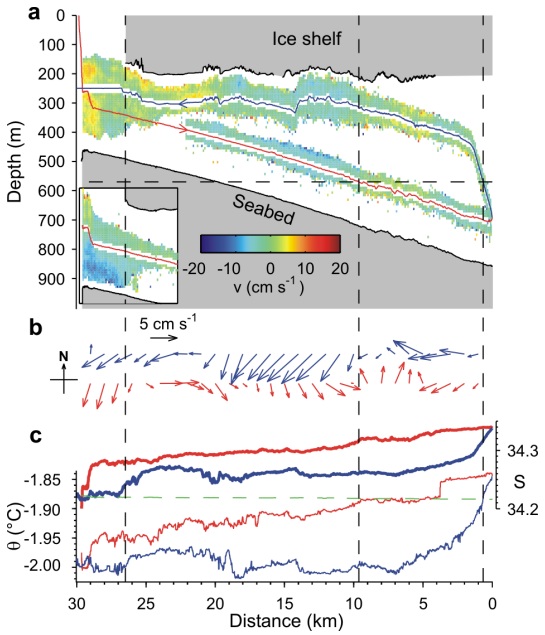

Figure 2. Oceanographic data from Mission 382. Red and blue lines indicate the outward and return legs, respectively. (a) Actual mission trajectory. The vertical broken line at 26.5 km gives the position of the ice front, referenced to the turning point in the mission; the horizontal broken line at 570 m depth shows the depth of the main sill at the continental shelf break (see Figure 1). Also shown are the ADCP data illustrating the dramatically reduced range beneath the ice shelf that implies a dearth of appropriately sized scatterers in the water column. The data are for the north-south velocity component (positive northward, approximately perpendicular to the ice front), which have been averaged using a horizontal window 100 m wide. The inset figure shows the ADCP data in the vicinity of the ice front for the outward leg. (b) Vertically averaged ADCP currents after subtraction of the modelled tide. (c) Salinity (bold), and potential temperature (θ). The thin, green, near-horizontal broken line is the freezing point of the water at surface pressure for salinities measured on the outward journey.

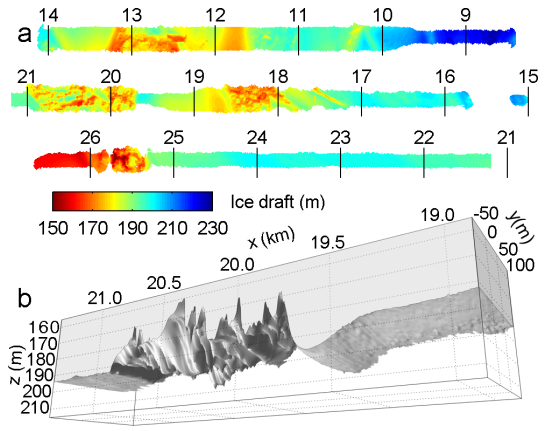

Figure 3. Multibeam data from the return leg. (a) Ice shelf draft (m), the track starting beneath the ice shelf (0 km) and ending at the ice front. The track of Autosub is indicated on the satellite image, cross-referencing the distance along the track in kilometers (Figure 1). (b) A 3D rendering shows a portion of the ice base below a flow trace at 20 km, including the smooth base either side of the feature.

[7] The salinity and temperature data from Autosub exhibit a wealth of detail (Figure 2c). Here we are concerned only with the main features of the records and what they can tell us about the large-scale circulation within the cavity. At the pressure of the base of the ice shelf (about 200 dbar; see Figure 2a) the freezing point of seawater is 0.15°C lower than at the surface [*Millero*, 1978]. The coldest water masses that can be generated at the sea surface outside of the cavity (~−1.9°C, the surface freezing point) are therefore always warmer than the melting point at the ice shelf base, and thus capable of powering basal melting. In polar regions the salinity is the dominant control on water density; the water closer to the ice shelf base is freshened and, largely incidental to the density, cooled in the process of melting the ice.

[8] A striking feature of the data presented in Figure 2 is the role played by the nearby main sill (Figure 1). The depth of the sill (about 570 m) is indicated in Figure 2a. From where this depth intersects Autosub's trajectory we see that the water deeper than the sill is either at, or warmer than, the surface freezing point (Figure 2c) calculated using the salinity measured by the vehicle. All the water sampled by Autosub above the depth of the sill has a temperature below the surface freezing point, and is therefore Ice Shelf Water (ISW) by definition [*Jacobs et al.*, 1970]. The de-tided water currents indicate a different circulation regime above (south-eastward) and below (north-westward) the sill depth (Figure 2b). Another obvious feature is the 0.02°C temperature increase in only 14 m along the outward track about 4 km before the turning point, a temperature front that marks the change to a different water mass whose maximum temperature is well above the surface freezing point. The presence of this warmer water implies some degree of exposure to the warmer waters found off the continental shelf. The potentially high basal melt rates that might result from this exposure are significant, as the ice shelves fringing the south eastern Weddell Sea are thought to play an important role in suppressing deep water formation in the region [*Fahrbach et al.*, 1994].

[9] We determine the warmer water's likely route into the cavity by comparing the data from Autosub with the conductivity-temperature-depth (CTD) data from stations occupied by the ship at the likely inflow sites along the ice front, identified as the main sill (CTD stations in orange) and the eastern sill (stations in green) in Figure 1. The orange stations sampled the westward flow along the shelf break to the east of the ice tongue, capturing the properties of water entering the cavity via the eastern slope of the main sill; the presence of the ice tongue prohibited us from sampling the waters over the eastern slope directly. Station 15 lies on the western slope of the main sill, sampling outflow from the cavity. Figure 4 shows the CTD data from these ice front stations plotted on a potential temperature - salinity (θ-S) diagram, together with the data from Autosub. The mixing lines included in the figure show how the θ-S characteristics of a water mass evolve when it interacts with ice; the lines are straight because, during melting or freezing, the change in the water's heat content is directly proportional to its change in salinity. The gradient of the mixing lines can be approximated by $L/(Sc_w)$ where L and c_w are the latent heat of fusion and specific heat capacity of ice, and S is the salinity of the ocean water below the upper boundary layer beneath the ice shelf [*Nøst and Foldvik*, 1994; *Gade*, 1979].

[10] From the mixing lines in Figure 4, none of the water types seen just east of the main sill (orange stations) are saline enough to be the source for any of the water observed during the mission. Thus the main sill was not the route into the cavity for the observed water masses. The mixing lines also show that both the warmer water measured by Autosub beyond the temperature front and below the depth of the main sill, and all the ISW from above the depth of the main sill, is most likely related to water flowing over the eastern

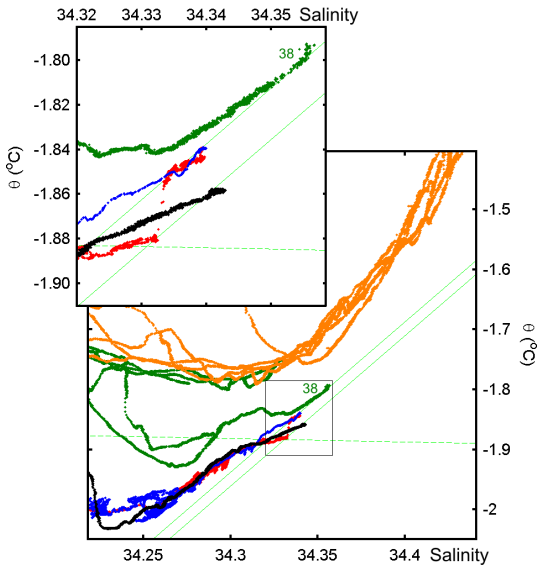

Figure 4. Potential temperature - salinity diagram showing data from CTD stations at the ice front, and those collected by Autosub. Station 15 (black), stations just east of ice tongue (orange), and stations near eastern sill (green) are included. The red markers are for Autosub's outward track, the blue are for the return leg. The near-horizontal broken line is the surface freezing point, and the straight sloping lines are mixing lines.

sill (green station 38). All but the deepest water seen exiting the cavity at Station 15 had the same properties as the ISW observed beneath the ice shelf, and was again most likely to have been derived from water of the properties observed at Station 38.

[11] The remaining water measured by Autosub, the water near the surface freezing point at and below the sill depth (between kilometer 9.5 and 4 on the inward leg) has a salinity between 34.32 and 34.33, and is characteristic of Eastern Shelf Water (ESW) [*Foldvik et al.*, 1985], a water mass formed as a result of the combined effects of wintertime sea ice production and glacial melt. As ESW was not observed anywhere over the continental shelf during the cruise it presumably entered the cavity during the previous winter. Another indication of unsteady ventilation of the cavity can be seen from the characteristics of the deepest water at Station 15. As this water is leaving the cavity, its parent water must have been warmer and more saline, that is, from further up the mixing line. Again, such a water type was not seen at any of the stations occupied during the cruise, suggesting that the cavity is subject to events of episodic flushing with warmer, more saline water.

[12] Easterly winds in the southern Weddell Sea cause a southward surface Ekman drift and a consequential deepening of the thermocline that separates the cold shallower waters from the warmer deeper water. The strength of the easterlies thus controls how near the warm water is to crossing the sill into the sub-ice shelf cavity [*Smedsrud et al.*, 2006]. A time-varying depth of the interface would be consistent with our conclusion that the cavity is episodically flushed with warmer waters. The huge Filchner-Ronne and Ross ice shelves are largely protected from the relatively warm waters beyond the continental shelf break by broad continental shelves. In contrast, Fimbul Ice Shelf is subject to extreme changes in regime that can result from relatively small changes in conditions at the continental shelf break: a quite minor change in the depth of the interface between the warmer and cooler water can lead to a dramatic change in the fortunes of the ice shelf.

4. Conclusions

[13] The principal conclusions from this first successful AUV deployment beneath an Antarctic ice shelf are that, beneath glaciological flow traces, the bases of Antarctic ice shelves are likely to be much rougher than hitherto thought, and that the cavity beneath Fimbul Ice Shelf, and probably other nearby ice shelves, is episodically flushed with relatively warm waters. Perhaps the most important finding from this mission is how much AUVs have to offer as platforms for sub-ice shelf exploration: a single mission has yielded a wealth of detail about the oceanography and topography of this fascinating environment.

References

Fahnestock, M. A., T. A. Scambos, R. A. Bindschadler, and G. Kvaran (2000), A millennium of variable ice flow recorded by the Ross Ice Shelf, Antarctica, *J. Glaciol.*, *46*, 652–664.

Fahrbach, E., R. G. Peterson, G. Rohardt, P. Schlosser, and R. Bayer (1994), Suppression of Bottom Water formation in the southeastern Weddell Sea, *Deep Sea Res., Part I*, *41*, 389–411.

Foldvik, A., T. Gammelsrød, and T. Tørresen (1985), Circulation and water masses on the Southern Weddell Sea Shelf, in *Oceanology of the Antarctic Continental Shelf*, *Antarct. Res. Ser.*, vol. 43, edited by S. S. Jacobs, pp. 5–20, AGU, Washington, D. C.

Gade, H. G. (1979), Melting of ice in sea water: A primitive model with application to the Antarctic ice shelf and icebergs, *J. Phys. Oceanogr.*, *9*, 189–198.

Jacobs, S. S., A. F. Amos, and P. M. Bruchhausen (1970), Ross Sea oceanography and Antarctic Bottom Water formation, *Deep Sea Res.*, *17*, 935–962.

Jenkins, A., and D. M. Holland (2002), A model study of ocean circulation beneath Filchner-Ronne Ice Shelf, Antarctica: Implications for bottom water formation, *Geophys. Res. Lett.*, *29*(13), 1634, doi:10.1029/2002GL015647.

Jones, D., B. Bett, S. McPhail, C. Flewellen, and M. Conquer (2005), Seabed photography from an autonomous underwater vehicle, *J. Mar. Sci. Environ.*, *C3*, 21–28.

Lythe, M. B., and D. G. Vaughan (2001), BEDMAP: A new ice thickness and subglacial topographic model of Antarctica, *J. Geophys. Res.*, *106*, 11,335–11,351.

MacAyeal, D. R. (1984), Numerical simulations of the Ross Sea tides, *J. Geophys. Res.*, *89*, 607–615.

Millard, N. W., G. Griffiths, G. Finegan, S. D. McPhail, D. T. Meldrum, M. Pebody, J. R. Perrett, P. Stevenson, and A. T. Webb (1998), Versatile autonomous submersibles—The realising and testing of a practical vehicle, *Underwater Tech.*, *23*, 7–17.

Millero, F. J. (1978), Freezing point of sea water, in *Eighth Report of the Joint Panel of Oceanographic Tables and Standards*, *UNESCO Tech. Pap. Mar. Sci.*, *28*, 29–31.

Nicholls, K. W., and K. Makinson (1998), Ocean circulation beneath the western Ronne Ice Shelf, as derived from in situ measurements of water currents and properties, in *Ocean, Ice, and Atmosphere: Interactions at the Antarctic Continental Margin*, *Antarct. Res. Ser.*, vol. 75, edited by S. S. Jacobs and R. F. Weiss, pp. 301–318, AGU, Washington, D. C.

Nøst, O. A. (2004), Measurements of ice thickness and seabed topography under the Fimbul Ice Shelf, Dronning Maud Land, Antarctica, *J. Geophys. Res.*, *109*, C10010, doi:10.1029/2004JC002277.

Nøst, O. A., and A. Foldvik (1994), A model of ice-shelf ocean interaction with application to the Filcher-Ronne and Ross Ice shelves, *J. Geophys. Res.*, *99*, 14,243–14,254.

Orsi, A. H., W. M. Smethie, and J. L. Bullister (2002), On the total input of Antarctic waters to the deep ocean: A preliminary estimate from chlorofluorocarbon measurements, *J. Geophys. Res.*, *107*(C8), 3122, doi:10.1029/2001JC000976.

Payne, A. J., A. Vieli, A. P. Shepherd, D. J. Wingham, and E. Rignot (2004), Recent dramatic thinning of largest West Antarctic ice stream triggered by oceans, *Geophys. Res. Lett.*, *31*, L23401, doi:10.1029/2004GL021284.

Raymond, M. J., and G. H. Gudmundsson (2005), On the relationship between surface and basal properties on glaciers, ice sheets and ice streams, *J. Geophys. Res.*, *110*, B08411, doi:10.1029/2005JB003681.

Scambos, T., B. Raup, and J. Bohlander (2005), Images of Antarctic ice shelves, http://www-nsidc.colorado.edu/data/nsidc-0102.html, Natl. Snow and Ice Data Cent., Boulder, Colo.

Smedsrud, L. H., A. Jenkins, D. M. Holland, and O. A. Nøst (2006), Modeling ocean processes below Fimbulisen, Antarctica, *J. Geophys. Res.*, *111*, C01007, doi:10.1029/2005JC002915.

Wadhams, P., J. P. Wilkinson, and S. D. McPhail (2006), A new view of the underside of Arctic sea ice, *Geophys. Res. Lett.*, *33*, L04501, doi:10.1029/2005GL025131.

E. P. Abrahamsen, K. W. Nicholls, and C. J. Pudsey, British Antarctic Survey, High Cross, Madingley Road, Cambridge CB3 0ET, UK. (kwni@bas.ac.uk)

J. J. H. Buck and G. F. Lane-Serff, School of Mechanical, Aerospace and Civil Engineering, University of Manchester, P.O. Box 88, Manchester M60 1QD, UK.

P. A. Dodd, C. Goldblatt, K. J. Heywood, K. I. C. Oliver, and M. R. Price, School of Environmental Sciences, University of East Anglia, Norwich NR4 7TJ, UK.

G. Griffiths, S. D. McPhail, N. W. Millard, J. Perrett, K. Saw, K. Stansfield, and A. T. Webb, National Oceanography Centre, European Way, Southampton SO14 3ZH, UK.

N. E. Hughes and J. P. Wilkinson, Scottish Society for Marine Sciences, Dunstaffnage Laboratory, Oban, Argyll PA37 1QA, UK.

A. Kaletzky and P. Wadhams, Department of Applied Mathematics and Theoretical Physics, Centre for Mathematical Sciences, University of Cambridge, Wilberforce Road, Cambridge CB3 0WA, UK.

M. J. Stott, Gregory Court, Churchfield Way, Wye, Kent TN25 5EG, UK.